Redox Biology 22 (2019) 101117

Contents lists available at ScienceDirect

Redox Biology

journal homepage: www.elsevier.com/locate/redox

Research Paper

(-)-Epicatechin attenuates hepatic sinusoidal obstruction syndrome by inhibiting liver oxidative and inflammatory injury

Zhenlin Huang[a,1], Xiaoqi Jing[a,b,1], Yuchen Sheng[b], Jiaqi Zhang[a], Zhanxia Hao[a], Zhengtao Wang[a], Lili Ji[a,*]

[a] The MOE Key Laboratory for Standardization of Chinese Medicines, Shanghai Key Laboratory of Compound Chinese Medicines and The SATCM Key Laboratory for New Resources and Quality Evaluation of Chinese Medicines, Institute of Chinese Materia Medica, Shanghai University of Traditional Chinese Medicine, Shanghai 201203, China

[b] Center for Drug Safety Evaluation and Research, Innovation Research Institute of Traditional Chinese Medicine, Shanghai University of Traditional Chinese Medicine, Shanghai 201203, China

ARTICLE INFO

Keywords:
(-)-Epicatechin
Monocrotaline
HSOS
Nrf2
NFκB

ABSTRACT

Hepatic sinusoidal obstruction syndrome (HSOS) is a rare liver disease with considerable morbidity and mortality. (-)-Epicatechin (EPI) is a natural flavonol. This study aims to investigate the protection of EPI against monocrotaline (MCT)-induced HSOS and its engaged mechanism. Results of serum alanine/aspartate aminotransferases (ALT/AST) activities, total bilirubin (TBil) and bile acids (TBA) amounts, liver histological evaluation, scanning electron microscope observation and hepatic metalloproteinase-9 (MMP-9) expression all demonstrated the protection by EPI against MCT-induced HSOS in rats. EPI attenuated liver oxidative injury induced by MCT. EPI enhanced the nuclear translocation of nuclear factor erythroid 2-related factor 2 (Nrf2) and increased the expression of its downstream antioxidant genes in rats. Molecular docking results implied the potential interaction of EPI with the Nrf2 binding site in kelch-like ECH-associated protein-1 (Keap1). The EPI-provided protection against MCT-induced HSOS was diminished in Nrf2 knock-out mice when mice were treated with MCT for 24 h but not for 48 h. However, EPI reduced the increased liver myeloperoxidase (MPO) activity, hepatic infiltration of immune cells, pro-inflammatory cytokines expression and nuclear factor κB (NFκB) activation in both wild-type and Nrf2 knock-out mice when mice were treated with MCT for 48 h. EPI reduced the elevated serum heat shock protein 60 (HSP60) content, and reversed the decreased mitochondria expression of HSP60 and Lon in livers from MCT-treated rats. Furthermore, the MCT-induced HSOS was markedly alleviated in mice treated with anti-HSP60 antibody. Taken together, this study demonstrates that EPI attenuates MCT-induced HSOS by reducing liver oxidative injury via activating Nrf2 antioxidant pathway and inhibiting liver inflammatory injury through abrogating NFκB signaling pathway initiated by HSP60.

1. Introduction

HSOS is a serious and life-threatening liver disease that usually arises within the first 30 days after hematopoietic stem-cell transplantation (HSCT), and its main clinical symptoms include painful hepatomegaly, jaundice, liver ascites and weight gain [1–3]. The severe HSOS is typically associated with multi-organ failure (MOF) and its mortality rate is higher than 80% [4,5]. Even for moderate HSOS, the mortality rate is still estimated at approximately 20% [6]. The intake of herbal medicines or teas containing hepatotoxic pyrrolizidine alkaloids

Abbreviations: ALT/AST, alanine/aspartate aminotransferases; DILI, drug-induced liver injury; EPI, (-)-epicatechin; GCLC, catalytic subunit of glutamate-cysteine ligase; GCLM, modify subunit of glutamate-cysteine ligase; GSH, reduced glutathione; GST, glutathione-S-transferase; H_2DCFDA, 2′-7′-dichlorodihydrofluorescein diacetate; H&E, hematoxylin-eosin; HSECs, hepatic sinusoidal endothelial cells; HO-1, heme oxygenase 1; HPAs, hepatotoxic pyrrolizidine alkaloids; HSCT, hematopoietic stem-cell transplantation; HSOS, hepatic sinusoidal obstruction syndrome; i.g., intragastrical administration; HSP60, heat shock protein 60; Keap1, kelch-like ECH-associated protein-1; LPO, lipid peroxidation; MCT, monocrotaline; MDA, malondialdehydeand; MMP-9, metalloproteinase-9; MOF, multi-organ failure; MPO, myeloperoxidase; NAFLD, nonalcoholic fatty liver disease; NFκB, nuclear factor κB; NQO1, NAD(P)H: quinone oxidoreductase 1; Nrf2, Nuclear factor erythroid 2-related factor 2; ROS, reactive oxygen species; TALEN, transcription activator-like effector nucleases; TBA, bile acids; TBil, total bilirubin

* Corresponding author.
E-mail addresses: lichenyue1307@126.com, jilili@shutcm.edu.cn (L. Ji).

[1] These two authors contributed equally to this work.

https://doi.org/10.1016/j.redox.2019.101117
Received 26 November 2018; Received in revised form 14 January 2019; Accepted 20 January 2019
Available online 14 February 2019

(HPAs) is another main cause for the development of HSOS. Since the first reported hepatotoxicity due to senecio poisoning, there are over thousands of clinical cases about HPAs-induced HSOS in the world, among which in China about hundreds of cases were caused by *gynura segetum* (Tusanqi) that contains abundant HPAs [7–9]. So HSOS due to HPAs intake shall arouse our attention. MCT, a retronecine-type HPA, is abundant in Crotalaria genus [10]. HSOS induced by MCT in rats has already been a classic animal model for experimental HSOS study [11,12].

The treatment for established HSOS is still very limited in clinic. Recently, the use of defibrotide is proposed for HSOS treatment due to its varying pharmacological activities including restoring thrombo-fibrinolytic balance, anti-inflammatory, anti-ischemic and anti-atherosclerotic activity, and its protection on endothelial cells [13–15]. However, the safety and efficacy of defibrotide still needs deep evaluation. Also, defibrotide is not a licensed drug in many countries, and its high acquisition cost has caused obstacles for its use in clinic.

Catechins, a type of natural polyphenols, are widely distributed in teas, coffee bean and various fruits including grape and apple [16]. Catechins have various pharmacological functions including anti-inflammatory, antioxidant and antithrombotic activities, and the reversal of endothelial dysfunction [17]. Catechins have four diastereoisomers, of which epicatechin is in cis-configuration. Of the two epicatechin isomers, (-)-epicatechin (EPI) is the most common isomer. EPI has well-known antioxidant and anti-inflammatory capacity, and it is useful for various diseases such as cancer, cardiovascular disease, diabetes, stroke and neurodegenerative diseases [18]. This study aims to observe the protection of EPI against MCT-induced HSOS and its engaged mechanism.

2. Materials and methods

2.1. Antibodies and reagents

MCT and EPI were both purchased from Sigma Chemical Co. (St. Louis, MO). Kits for detecting malondialdehyde (MDA) and reduced glutathione (GSH) amount, MPO and glutathione-S-transferase (GST) activities, and for isolating mitochondrial proteins were purchased from Nanjing Jiancheng Bioengineering Institute (Nanjing, China). Antibodies for MMP-9, NFκB, IκB, p-IκB, Lamin B1, COXIV and β-actin were purchased from Cell Signaling Technology (Danvers, MA). Antibodies for Nrf2, catalytic/modify subunit of glutamate-cysteine ligase (GCLC/GCLM), heme oxygenase-1 (HO-1), NAD(P)H: quinone oxidoreductase 1 (NQO1) were obtained from Santa Cruz (Santa Cruz, CA). Antibodies for HSP60 and Lon were purchased from GeneTax Inc. (Alton Parkway Irvine, CA). Antibody for TLR4 was purchased from Biobasic Inc (Shanghai, China). Peroxidase-conjugated goat anti-Rabbit IgG (H + L) and anti-Mouse IgG (H + L) were purchased from Jackson ImmunoResearch (West Grove, PA). Enhanced chemiluminescence kits were obtained from Millipore (Darmstadt, Germany). HSP60 blocking antibody and control IgG were obtained from Abcam (Cambridge, MA). NE-PER nuclear and cytoplasmic extraction reagents, and BCA protein assay kits were purchased from ThermoFisher Scientific (Waltham, MA). 2′-7′-dichlorodihydrofluorescein diacetate (H_2DCFDA), Immunoprecipitation kits and Trizol were all bought from Life Technology (Carlsbad, CA). PrimeScript Master Mix and SYBR Premix Ex Taq were bought from Takara (Shiga, Japan). DAKO EnVision detection system was purchased from DAKO Corporation (Carpinteria, CA). Other reagents unless indicated were purchased from Sigma Chemical Co. (St. Louis, MO).

2.2. Experimental animals

Specific pathogen free male Sprague-Dawley rats (200–240 g) and C57BL/6 male mice (16–20 g) were bought from Shanghai Laboratory Animal Center of Chinese Academy of Science (Shanghai, China). Nrf2 knock-out (*Nrf2*$^{-/-}$) C57BL/6 mice were generated by SiDanSai Biotechnology Inc (Shanghai, China) by using transcription activator-like effector nucleases (TALEN) technology [19]. A pair of TALEN constructs for Nrf2 knock-out were cloned into a mammalian expression vector pCMV-TALEN and capped, polyA-tailed mRNA for injection were produced using the Ambion mMessage mMachine kits. The C57BL/6 knock-out mice were produced by micro-injecting TALEN mRNAs into fertilized eggs. The knock-out allele has been sequence validated to have two missing base pairs (GA, 346–347 of the ORF), causing a frame shift and an early stop. DNA isolated from tail biopsies was used for genotyping.

Experimental animals were fed with a standard laboratory diet and given free access to tap water. Animals were housed in a specific pathogen-free facility with controlled room temperature (22 ± 1 °C), humidity (65 ± 5%) with 12:12 h light/dark cycle. All animals have received humane care in compliance with the institutional animal care guidelines approved by the Experimental Animal Ethical Committee of Shanghai University of Traditional Chinese Medicine (Approval Number: 201510003, 201612010).

2.3. Animal treatment

Rats were divided into five groups as following: (1) Vehicle control (n = 9), (2) MCT (n = 11), (3) MCT + EPI (20 mg/kg) (n = 10), (4) MCT + EPI (40 mg/kg) (n = 10), (5) EPI (40 mg/kg) (n = 6). Rats were orally administered with MCT (90 mg/kg, intragastrical administration, i.g.) or vehicle for once, and then were given with EPI (20 or 40 mg/kg, i.g.) twice at 5 h and 29 h after MCT administration. Rats were sacrificed at 48 h after MCT administration, and blood and livers were collected.

Nrf2$^{+/+}$ and *Nrf2*$^{-/-}$ C57BL/6 male mice were randomly divided into three groups, respectively. (1) Vehicle control (n = 20), (2) MCT (n = 22), (3) MCT + EPI (n = 22). Mice were orally administered with MCT (360 mg/kg, i.g.) or vehicle for once, and then were given with EPI (40 mg/kg, i.g.) twice at 5 h and 29 h after MCT administration. Mice were sacrificed at 24 h or 48 h after MCT administration, and blood and livers were collected.

C57BL/6 mice were randomly divided into four groups: (1) vehicle control (n = 5), (2) 360 mg/kg MCT (n = 5), (3) 360 mg/kg MCT + anti-HSP60 antibody (n = 5), (4) 360 mg/kg MCT + control IgG (n = 5). Anti-HSP60 blocking antibody or control IgG were tail intravenously injected into mice (10 μg, 10 min prior to MCT administration) respectively. At 48 h after MCT administration, mice were sacrificed, blood and livers were collected.

2.4. Serum biochemistry analysis

Fresh blood was obtained and kept at room temperature for 1 h. Serum was collected after centrifugation at 850 × *g* for 15 min. Serum ALT/AST activity, total TBil and TBA amounts were determined with an automatic biochemical analyzer (HITACHI 7080, Japan).

2.5. Blood cell analysis

Fresh blood was collected from rats of each group by using anticoagulant solution. Blood cells were analyzed by using BAYER ADVIA-120 (German).

2.6. Liver histological observation

A piece of the liver was fixed and embedded in paraffin, and subsequently sectioned (5 μM) and stained with hematoxylin-eosin (H&E), and then observed under a microscope (Olympus, Japan).

2.7. Scanning electron microscope evaluation

Three rats or mice in each group were firstly perfused with phosphate buffered saline through the hepatic portal vein, and then perfused with a fixative solution containing 2.5% glutaraldehyde. Livers were further cut into small pieces (approximately 5 mm^3), and each sample was ion-sputter-coated and observed under a scanning electron microscopy (Hitachi S-4700).

2.8. Measurement of liver lipid peroxidation (LPO) and GSH amounts

MDA, formed as the product of LPO, was served as an index for reflecting LPO. MDA and GSH amounts were determined by using commercial kits and expressed as nmol/mg protein.

2.9. Measurement of liver GST activity

Liver GST activity was determined by using commercial kits and expressed as U/mg protein.

2.10. Real-time PCR analysis

Total RNA was extracted from livers by using TRIZOL reagent. cDNA was synthesized and Real-time PCR was performed. Relative expression of target genes was standardized to Actin, evaluated by $2^{-\Delta\Delta Ct}$ method and given as ratio of control. The primer sequences are shown in Table 1.

2.11. Western-blot analysis

Cytosolic and nuclear proteins in livers were isolated as described in kits. The protein concentration of each sample was detected and normalized to the equal protein concentration. For detecting the amount of HSP60 in serum, collected serum were directly mixed with protein loading buffer. Protein samples were separated by SDS-PAGE and blots were probed with appropriate combination of primary and horseradish peroxidase-conjugated secondary antibodies. Proteins were visualized by using enhanced chemiluminescence kits. The gray densities of the protein bands were normalized by using β-actin, Lamin B1 or COXIV as internal controls, and the results were expressed as fold of control. Ponceau red-stained proteins in the whole membrane were used as the loading control for detecting HSP60 in serum.

Table 1
List of Primers for Real-time PCR.

	Target	Gene ID	Primer	Sequence
rat	Hmox1	24451	FP	5'-TCCCGAACATCGACAGCCCCA-3'
			RP	5'-AGGGGCAGTATCTTGCACCAGG-3'
	Nqo1	24314	FP	5'-CAAGTTTGGCCTCTCTGTGG-3'
			RP	5'-AAGCTGCGTCTAACTATATGT-3'
	Actb	81822	FP	5'-TTCGTTGCCGGTCCACACCC-3'
			RP	5'-GCTTTGCACATGCCGGAGCC-3'
	Nfe2l2	83619	FP	5'-TCCTCTGCTGCCATTAGTCA-3'
			RP	5'-GTGCCTTCAGTGTGCTTCTG-3'
	Gclc	25283	FP	5'-TGAGGATGAGGAGGCATCAA-3'
			RP	5'-ACTGCAGGCTTGGAATGTCA-3'
	Gclm	29739	FP	5'-TTGCTATAGGCACCTCGGATCT-3'
			RP	5'-ATCTGGTGGCATCACACAGC-3'
	Hspd1	63868	FP	5'-CACCACCACTGCCACTGTTC-3'
			RP	5'-CCACAGCCAACATCACACCT-3'
	Lonp1	170916	FP	5'-GGAGCGCATGTACGAAGTCA-3'
			RP	5'-TGTCCTCCTTGCTGCCACTA-3'
mouse	Tnfa	21926	FP	5'-CACCCCGAAGTTCAGTAGACA-3'
			RP	5'-TCCCTCCAGAAAAGACACCAT-3'
	Il-6	16193	FP	5'-GTCACCAGCATCAGTCCCAAG-3'
			RP	5'-CCCACCAAGAACGATAGTCAA-3'
	Il1b	16176	FP	5'-TGTGTTTTCCTCCTTGCCTCTGAT-3'
			RP	5'-TGCTGCCTAATGTCCCCTTGAAT-3'
	Actb	11461	FP	5'-TTCGTTGCCGGTCCACACCC-3'
			RP	5'-GCTTTGCACATGCCGGAGCC-3'

FP, Forward Primer; RP, Reverse Primer.

2.12. Measurement of hepatic reactive oxygen species (ROS)

Hepatic ROS level was measured as described in our previous published paper [20]. The results were calculated as units of fluorescence per microgram of protein and presented as the percentage of control.

2.13. Molecular docking analysis

Molecular docking analysis was performed as described in our previous study [21]. The confirmation of EPI is generated using Conformational Search (MMFF94X force field) in MOE2013.

2.14. Measurement of liver MPO activity

Liver MPO activity was determined according to the manufacturer's instruction and expressed as units/g protein.

2.15. Immunohistochemical staining

Paraffin-embedded liver sections were deparaffinized in xylene and rehydrated in a gradient of ethanol to distilled water, and then quenched with 3% hydrogen peroxide and incubated with 5% bovine serum albumin, and then incubated with CD11b or Gr-1 antibodies at 4 °C overnight and further detected by using DAKO EnVision detection kits. Sections were counterstained with hematoxylin. The images were taken using an inverted microscope under the magnification of 200×. CD11b or Gr-1 positive cells were counted manually in three random fields in per sample (each group contains three samples).

2.16. Immunoprecipitation assay

Mitochondrial proteins in rats were extracted by using kits and protein concentration was detected, and then equal amounts of protein were subjected to immunoprecipitation with anti-HSP60 antibody as described in the kits. The immunoprecipitation was separated via SDS-PAGE and the conjugates were detected with anti-Lon and anti-HSP60 antibodies.

2.17. Statistical analysis

Data were expressed as means ± SEM. Groups were compared by one-way ANOVA, followed by *post hoc* LSD test when ANOVA found a significant value of F and no variance in homogeneity, otherwise, Mann-Whitney U nonparametric ANOVA was performed for analysis among groups. $P < 0.05$ was taken to indicate significant differences between group means.

3. Results

3.1. EPI attenuated MCT-induced HSOS in rats

As shown in Fig. 1A–D, EPI (40 mg/kg) decreased the elevated serum ALT and AST activities, and the increased TBil and TBA amounts induced by MCT (90 mg/kg) in rats. EPI (20 mg/kg) also reduced the increased serum TBil amount induced by MCT in rats (Fig. 1D). Liver histological observation showed that MCT induced severe liver damages, including intrahepatic hemorrhage, hepatic infiltration of immune cells, necrosis of hepatocytes, the dilatation of hepatic sinusoids, the detachment of hepatic sinusoidal endothelial cells (HSECs) and the destruction of liver structure (Fig. 1E–b). EPI (40 mg/kg) reversed all those phenomena (Fig. 1E–d), but the amelioration of EPI (20 mg/kg)

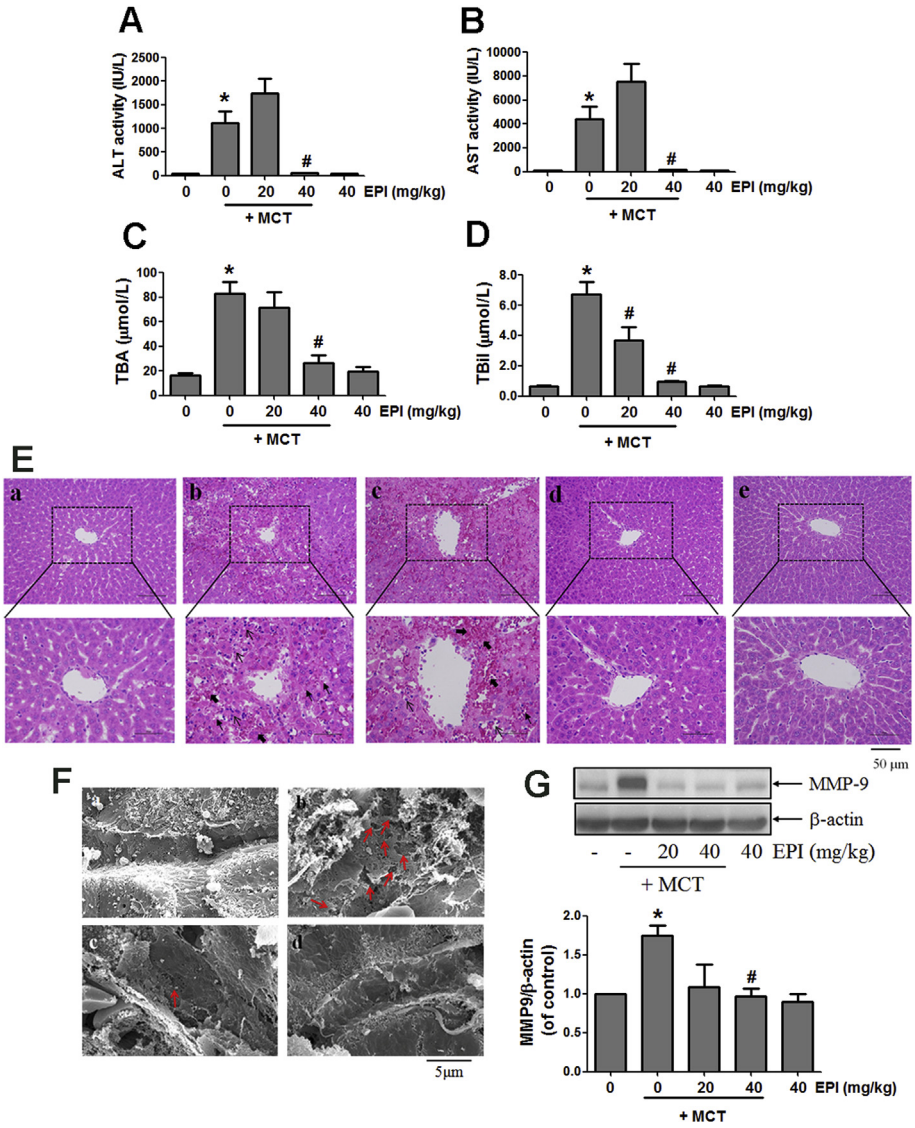

Fig. 1. EPI attenuated MCT-induced HSOS in rats. (A) Serum ALT activity (n = 5–8). (B) Serum AST activity (n = 5–8). (C) Serum TBA amount (n = 5–8). (D) Serum TBil amount (n = 5–8). (E) Histological observation of liver injury. (original magnification ×100, upper; partial enlarged pictures, down. The arrows indicate intrahepatic hemorrhage, indicate necrosis of hepatocytes, indicate hepatic infiltration of immune cells). a. Control, b. MCT, c. MCT + EPI (20 mg/kg), d. MCT + EPI (40 mg/kg), e. EPI (40 mg/kg). (F) Scanning electron microscopy observation. (Red arrows indicate the enlargement of fenestrate, exposure of the Disse space and the damage of endothelium). a. Control, b. MCT, c. MCT + EPI (20 mg/kg), d. MCT + EPI (40 mg/kg). (G) Hepatic MMP-9 expression was detected. Below figure is the quantitative densitometric analysis of MMP-9 protein (n = 5). Data are expressed as mean ± SEM. $^{*}P < 0.05$ versus control; $^{\#}P < 0.05$ versus MCT.

was weak (Fig. 1E–c). There is no liver damage occurred in control and EPI (40 mg/kg)-treated rats (Fig. 1E-a,e).

Scanning electron microscopy was used to further evaluate the potential damage on HSECs. As shown in Fig. 1F-b, MCT induced the dilatation of sinusoids, the enlargement of fenestrate, the exposure of Disse space and the damage on endothelium in rats. However, all those phenomena were ameliorated in rats treated with EPI (20, 40 mg/kg) (Fig. 1F-c,d). Also, there is no those above changes occurred in normal control rats (Fig. 1F–a). Further results showed that EPI (40 mg/kg) reduced the elevated expression of hepatic MMP-9 induced by MCT in rats (Fig. 1G).

MCT increased the number of rats with liver ascites (Table 2). EPI (40 mg/kg) reduced this increase, but EPI (20 mg/kg) had no inhibition (Table 2). Data in Table 3 showed that EPI (40 mg/kg) reversed the decreased number of platelets, reticulocytes, white blood and red cells induced by MCT in rats.

3.2. EPI reversed the MCT-induced liver oxidative injury in rats

Data in Fig. 2A and B showed that MCT (90 mg/kg) elevated liver MDA amount and ROS level in rats, but EPI (40 mg/kg) reduced this increase. EPI (40 mg/kg) alone had no obvious effects on liver MDA amount and ROS level in rats. MCT weakly increased hepatic GSH content and EPI (40 mg/kg) further enhanced this increase in rats (Fig. 2C). Additionally, EPI (40 mg/kg) alone obviously enhanced liver GSH content in rats. MCT reduced liver GST activity in rats, but EPI (40 mg/kg) reversed this decrease (Fig. 2D). EPI (40 mg/kg) alone had no obvious effect on liver GST activity in rats.

Table 2
The number of rats with liver ascites.

Group	Number of rats with ascites	Number of each group	Percentage of rats with ascites (%)
Vehicle control	0	9	0
MCT (90 mg/kg)	6	11	54.5
MCT + EPI (20 mg/kg)	8	10	80
MCT + EPI (40 mg/kg)	0	10	0
EPI (40 mg/kg)	0	6	0

Table 3
Changes in blood cell counts.

Group	PLT ($\times 10^9$/L)	RET ($\times 10^9$/L)	WBC ($\times 10^9$/L)	RBC ($\times 10^{12}$/L)
Vehicle	1234.3 ± 69.2	773.2 ± 41.9	6.5 ± 0.7	6.7 ± 0.1
MCT	57.4 ± 4.8***	274.6 ± 16.3***	1.6 ± 0.3***	4.9 ± 0.2***
MCT + EPI (20 mg/kg)	162.7 ± 89.4	366.4 ± 47.8##	3.7 ± 1.1	5.3 ± 0.2
MCT + EPI (40 mg/kg)	1011.0 ± 140.5###	510.3 ± 46.2##	4.9 ± 0.6###	6.9 ± 0.2###
EPI (40 mg/kg)	1379.3 ± 78.4	691.7 ± 49.2	5.4 ± 0.8	7.3 ± 0.3

MCT: Monocrotaline, EPI: (-)epicatechin, PLT: platelet, RET: reticulocyte, WBC: white blood cell, RBC: red cell.
***$P < 0.001$ versus Vehicle control, ##$P < 0.01$, ###$P < 0.001$ versus MCT.

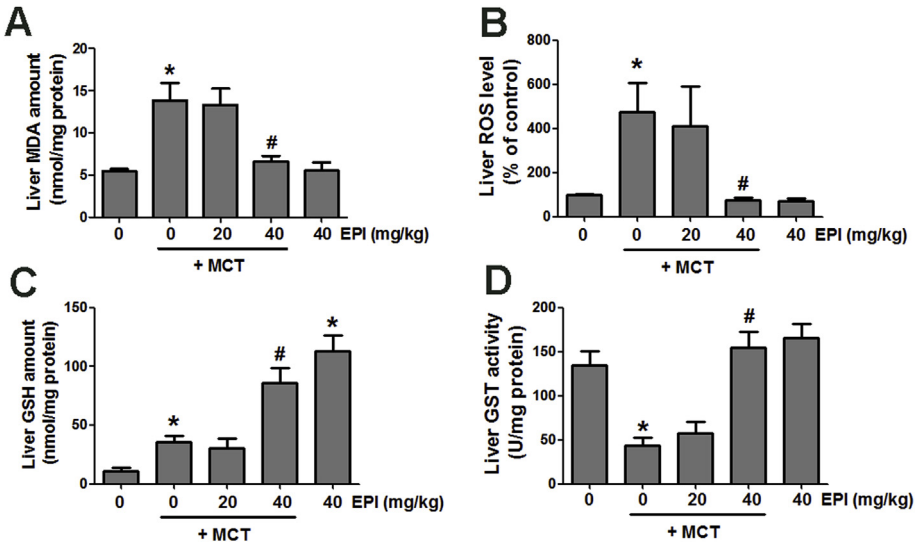

Fig. 2. EPI attenuated MCT-induced liver oxidative stress injury in rats. (A) MDA amount (n = 6). (B) ROS level (n = 6). (C) GSH amount (n = 6). (D) GST activity (n = 6). Data are expressed as mean ± SEM. *$P < 0.05$ versus control; #$P < 0.05$ versus MCT.

3.3. EPI induced the activation of Nrf2 antioxidant signaling pathway in rats

As shown in Fig. 3A, EPI (40 mg/kg) reversed the decreased hepatic Nrf2 mRNA expression induced by MCT (90 mg/kg) in rats. MCT reduced hepatic expression of Nrf2 protein in both cytosol and nucleus, but EPI (40 mg/kg) reversed this decrease (Fig. 3B and C). EPI (40 mg/kg) reversed the MCT-induced decrease in hepatic mRNA expression of GCLC, GCLM and NQO1 in rats (Fig. 3D). MCT increased HO-1 mRNA expression, but EPI (40 mg/kg) reduced this increase (Fig. 3E). Western-blot results showed that EPI (20, 40 mg/kg) increased GCLC protein expression in rats treated with MCT (Fig. 3F and G). EPI (40 mg/kg) reversed the reduced hepatic expression of GCLM and NQO1 induced by MCT in rats. EPI (20 mg/kg) also reversed the reduced NQO1 expression induced by MCT (Fig. 3F and G). As same as the results from mRNA expression, EPI (40 mg/kg) reduced the MCT-induced increase in HO-1 expression in rats (Fig. 3F and G).

3.4. Results of molecular docking analysis

The molecular docking analysis was conducted to detect the potential binding of EPI (chemical structure was shown in Fig. 4A) to the kelch domain of kelch-like ECH-associated protein-1 (Keap1). The docking mode of EPI in the Nrf2 binding site of Keap1 protein was illustrated in Fig. 4B (Front view) and Fig. 4C (Top View). The three-dimension (Fig. 4D) and two-dimension (Fig. 4E) interaction-map showed that EPI had an H-Bond interaction between the Ser508 bridging by one water molecule, and other one H-Bond interaction with Asn382. All those interactions help EPI anchored in the Nrf2 binding site of Keap1 protein.

3.5. Nrf2 was critical for regulating the EPI-provided protection against MCT-induced HSOS at the early stage

As shown in Fig. 5A–D, when mice were treated with MCT (360 mg/kg) for 24 h, there was no obvious elevation in serum ALT/AST activities, and TBil and TBA amounts in wild-type mice treated with MCT or MCT plus EPI. However, when Nrf2 knock-out mice were treated with MCT for 24 h, serum ALT/AST activities, and TBil and TBA amounts were all significantly increased (Fig. 5A–D). EPI (40 mg/kg) had no reduction on MCT-induced this increase in Nrf2 knock-out mice (Fig. 5A–D). When Nrf2 knock-out mice were treated with MCT for 24 h, MCT enhanced haptic ROS formation, but EPI had no inhibition on this increase (Fig. 5E). Moreover, serum ALT/AST activities, serum TBil and TBA amounts, and hepatic ROS level were all significantly higher in Nrf2 knock-out mice than in wild-type mice treated with MCT. Data in Fig. 5F confirmed the deletion of Nrf2 protein in Nrf2 knock-out mice.

Liver histological observation showed that when Nrf2 knock-out mice were treated with MCT for 24 h, MCT induced obvious liver damages including hepatic infiltration of immune cells, intrahepatic hemorrhage, necrosis of hepatocytes, the dilatation of hepatic sinusoids and the detachment of HSECs (Fig. 5G). EPI had no amelioration on these pathological lesions induced by MCT in Nrf2 knock-out mice. Weak liver damages occurred in wild-type mice treated with MCT for 24 h, including intrahepatic hemorrhage, hepatic infiltration of immune cells and necrosis of hepatocytes. Meanwhile, EPI ameliorated all these pathological lesions induced by MCT in wild-type mice.

Scanning electron microscopy observation showed that when Nrf2 knock-out mice were treated with MCT for 24 h, MCT induced the enlargement of fenestrate, the exposure of Disse space and the damage on endothelium (Fig. 5H). EPI had no amelioration on these pathological

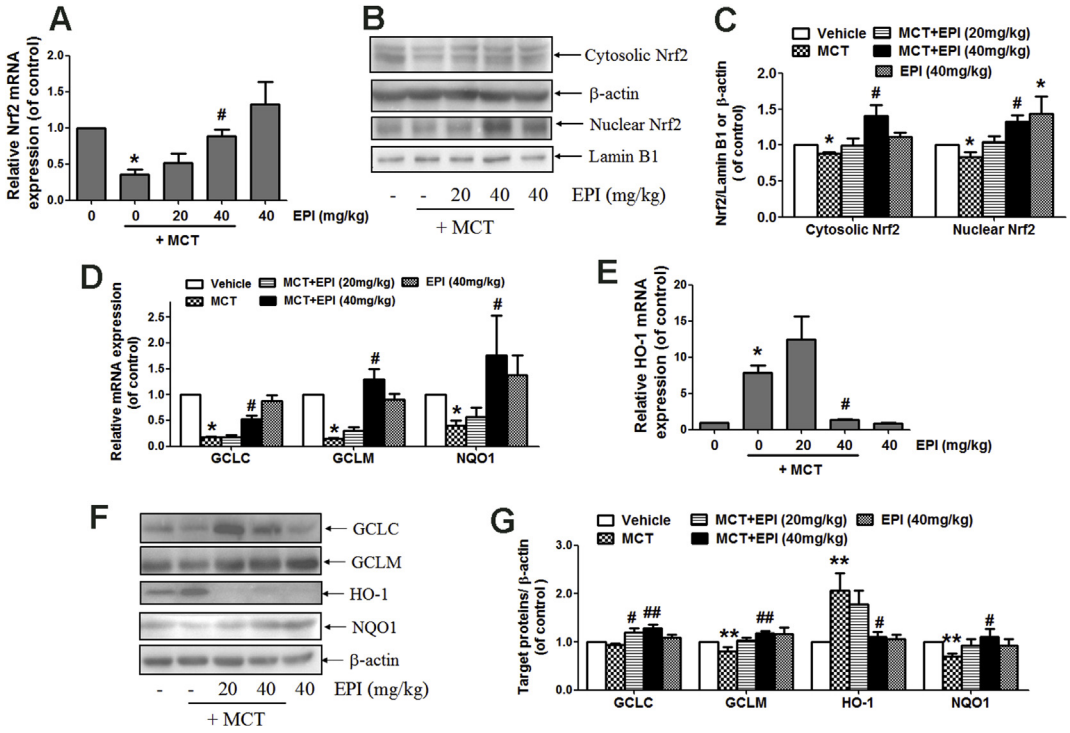

Fig. 3. EPI induced the activation of hepatic Nrf2 antioxidant signaling pathway in rats. (A) Nrf2 mRNA expression (n = 6). (B) Hepatic expression of cytosolic and nuclear Nrf2. (C) The quantitative densitometric analysis of Nrf2 protein (n = 5). (D) Hepatic mRNA expression of GCLC, GCLM and NQO1 (n = 6). (E) Hepatic HO-1 mRNA expression (n = 6). (F) Hepatic GCLC, GCLM, NQO1 and HO-1 protein expression. (G) The quantitative densitometric analysis of GCLC, GCLM, NQO1 and HO-1 (n = 5). Data are expressed as mean ± SEM. $^{*}P < 0.05$ versus control; $^{\#}P < 0.05$ versus MCT.

lesions induced by MCT in Nrf2 knock-out mice. When wild-type mice were treated with MCT for 24 h, MCT induced the enlargement of fenestrate and the exposure of Disse space, and all these pathological lesions were diminished in EPI-treated mice (Fig. 5H).

3.6. Nrf2 was not critically involved in regulating the EPI-provided protection against MCT-induced HSOS at the later stage

When wild-type and Nrf2 knock-out mice were treated with MCT (360 mg/kg) for 48 h, MCT induced obvious liver injury that is evidenced by the increased serum ALT/AST activities and TBil and TBA amounts, but EPI (40 mg/kg) reduced this increase in both wild-type and knock-out mice (Fig. 6A–D). When wild-type and Nrf2 knock-out mice were treated with MCT for 48 h, MCT elevated liver MDA amount, but EPI reduced this elevation in both wild-type and Nrf2 knock-out mice (Fig. 6E). Moreover, the EPI-provided protection is almost the same in wild-type and Nrf2 knock-out mice (Fig. 6A–E).

Liver histological evaluation showed that MCT induced obvious liver damages including intrahepatic hemorrhage, hepatic infiltration of immune cells, necrosis of hepatocytes, the dilatation of hepatic sinusoids and the detachment of HSECs in both wild-type and Nrf2 knock-out mice when mice were treated with MCT for 48 h (Fig. 6F).

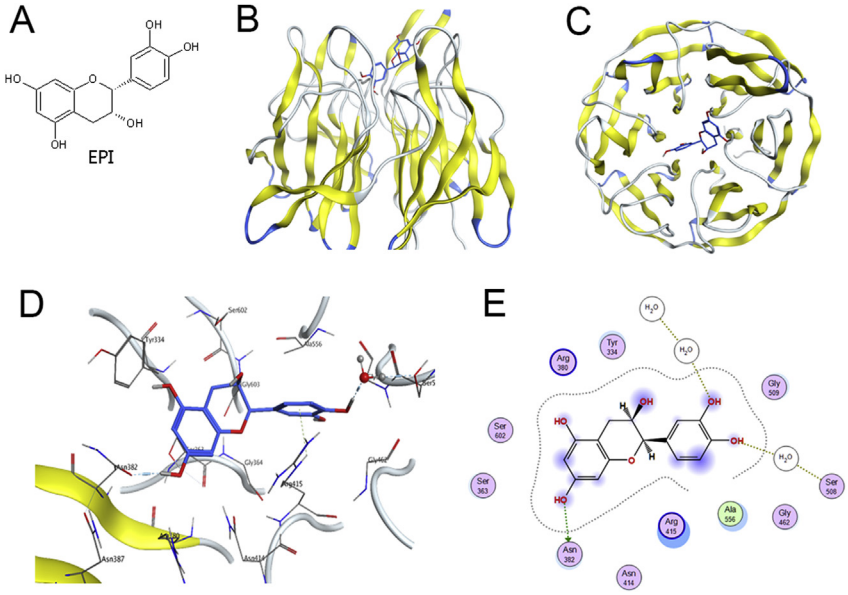

Fig. 4. Results of molecular docking analysis. (A) The chemical structure of EPI. (B) Front view of the docking mode of EPI (Blue) in the Nrf2 binding site of Keap1 protein (show in ribbon representation and colored by structure). (C) Top view of the docking mode of EPI (Blue) in the Nrf2 binding site of Keap1 (show in ribbon representation and colored by structure). (D) Representative amino acid residues surrounding EPI (Blue) in the Nrf2 binding pocket of Keap1. (E) Two-dimensional interaction map of EPI and the human Keap1. The arrows indicate potential interactions between amino acid residues and EPI.

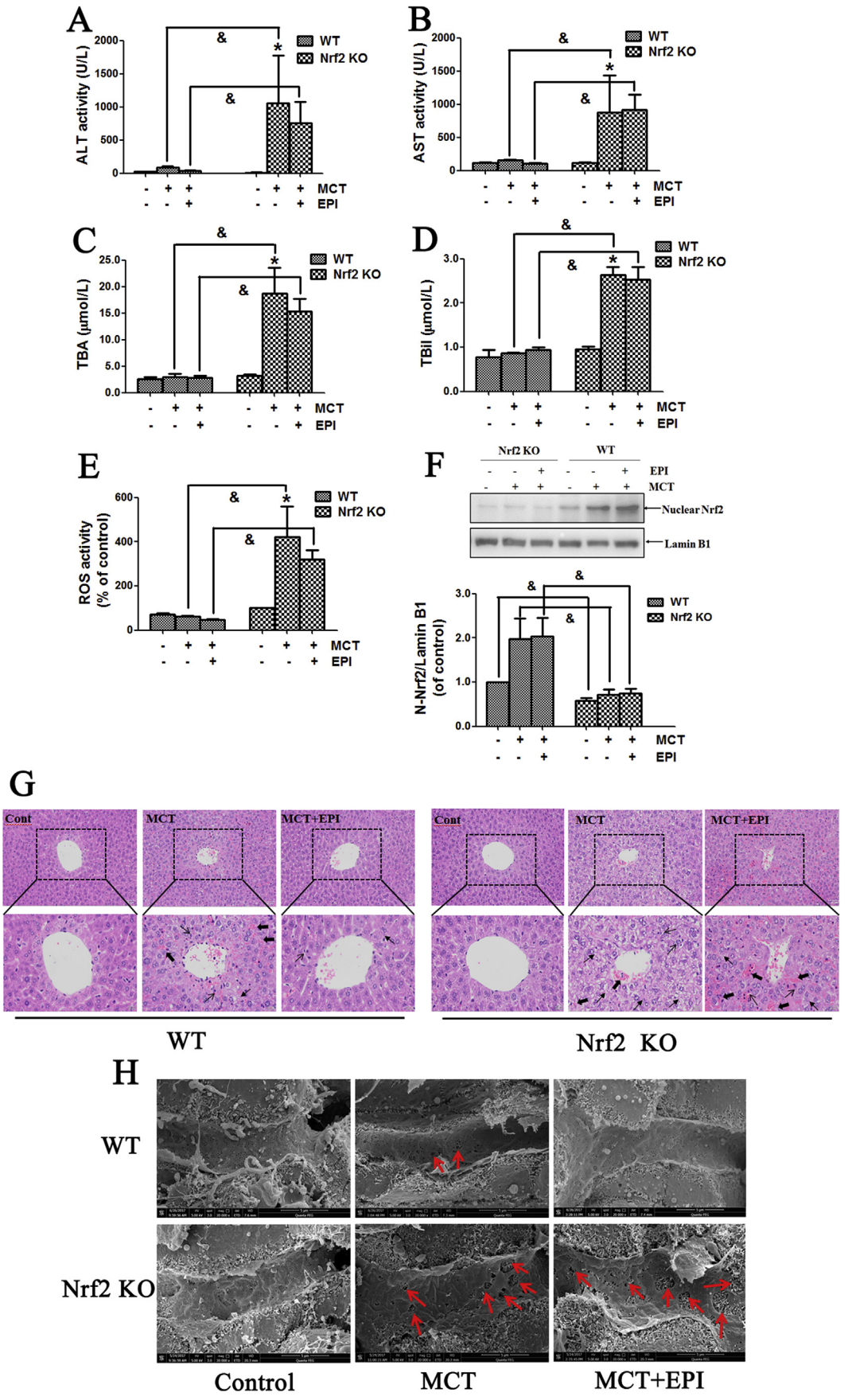

(caption on next page)

Fig. 5. Nrf2 was critical for regulating the EPI-provided protection against MCT-induced HSOS at the early stage. Wild-type or Nrf2 knock-out mice were given with MCT (360 mg/kg) and EPI (40 mg/kg), and sacrificed at 24 h after MCT administration. (A) Serum ALT activity (n = 6). (B) Serum AST activity (n = 6). (C) Serum TBA amount (n = 6). (D) Serum TBil amount (n = 6). (E) Hepatic ROS level (n = 6). (F) Hepatic Nrf2 expression. Below figure is the quantitative densitometric analysis of Nrf2 protein (n = 5). (G) Histological observation of liver injury. (original magnification ×100, upper; partial enlarged pictures, down. The arrows indicate intrahepatic hemorrhage, indicate necrosis of hepatocytes, indicate hepatic infiltration of immune cells). (H) Scanning electron microscopy observation. (Red arrows indicate the enlargement of fenestrate, exposure of the Disse space and the damage of endothelium). Data are expressed as mean ± SEM. $^{*}P < 0.05$ versus control; $^{\&}P < 0.05$ versus wild-type mice.

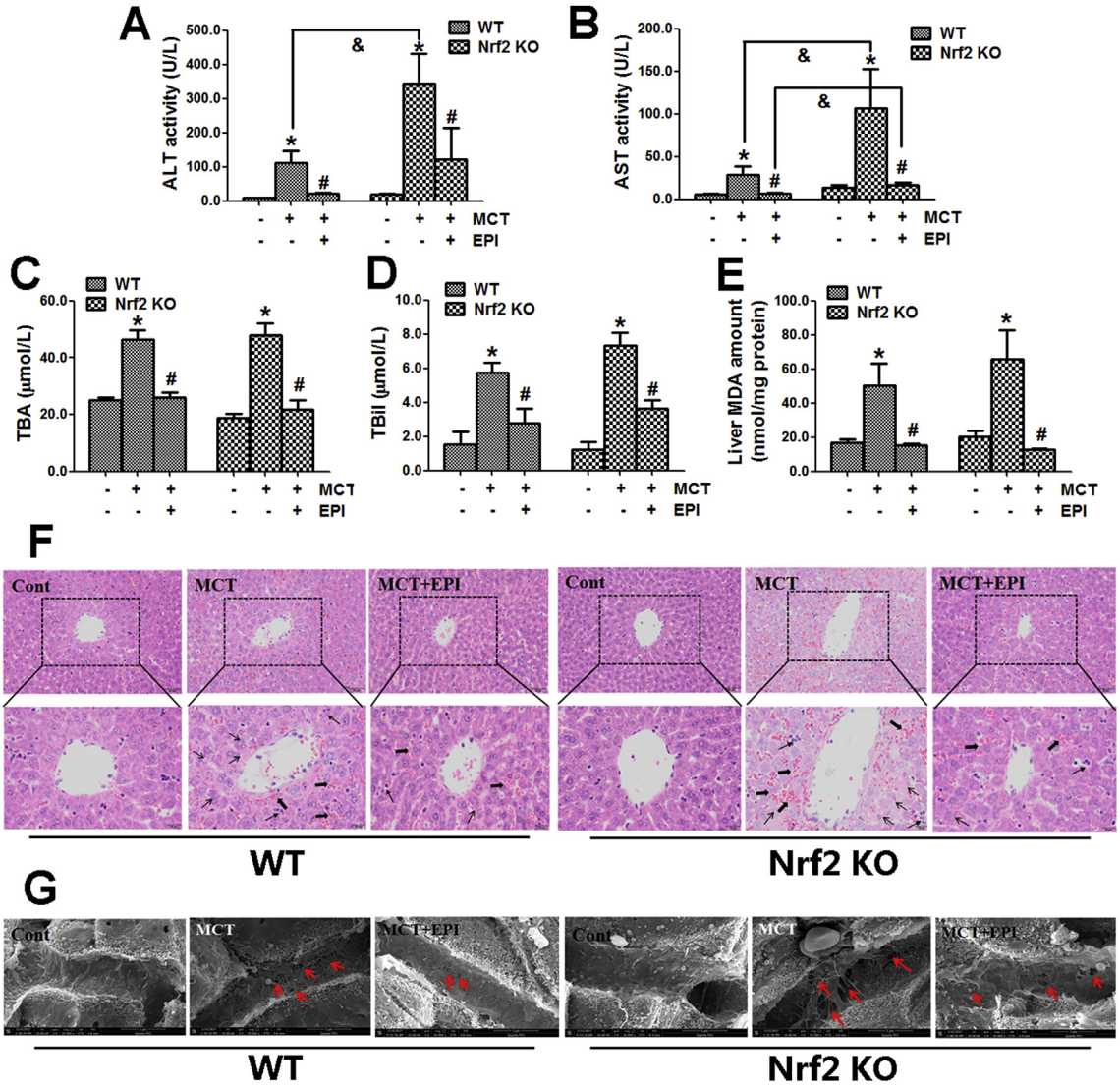

Fig. 6. Nrf2 was not critically involved in regulating the EPI-provided protection against MCT-induced HSOS at the later stage. Wild-type or Nrf2 knock-out mice were given with MCT (360 mg/kg) and EPI (40 mg/kg), and sacrificed at 48 h after MCT administration. (A) Serum ALT activity (n = 6). (B) Serum AST activity (n = 6). (C) Serum TBA amount (n = 6). (D) Serum TBil amount (n = 6). (E) Liver MDA amount (n = 6). (F) Histological observation of liver injury. (original magnification ×100, upper; partial enlarged pictures, down. The arrows indicate intrahepatic hemorrhage, indicate necrosis of hepatocytes, indicate hepatic infiltration of immune cells). (G) Scanning electron microscopy observation. (Red arrows indicate the enlargement of fenestrate, exposure of the Disse space and the damage of endothelium). Data are expressed as mean ± SEM. $^{*}P < 0.05$ versus control; $^{\#}P < 0.05$ versus MCT; $^{\&}P < 0.05$ versus wild-type mice.

EPI ameliorated all those pathological lesions in both wild-type and Nrf2 knock-out mice when mice were treated with MCT for 48 h.

Scanning electron microscopy observation showed that when wild-type or Nrf2 knock-out mice were treated with MCT for 48 h, MCT induced the enlargement of fenestrate, the exposure of Disse space and the damage on endothelium (Fig. 6G). EPI ameliorated all these pathological lesions induced by MCT in both wild-type and Nrf2 knock-out mice.

3.7. EPI attenuated liver inflammatory injury induced by MCT in Nrf2 knock-out mice

When wild-type and Nrf2 knock-out mice were treated with MCT (360 mg/kg) for 48 h, MCT enhanced liver MPO activity in both wild-type and Nrf2 knock-out mice. However, EPI (40 mg/kg) reduced this increase in both wild-type and Nrf2 knock-out mice (Fig. 7A).

MCT decreased hepatic IκB protein expression, and increased the expression of phosphorylated IκB and nuclear translocation of NFκB in both wild-type and Nrf2 knock-out mice when mice were treated with MCT for 48 h (Fig. 7B–E). EPI reversed all these phenomena in both

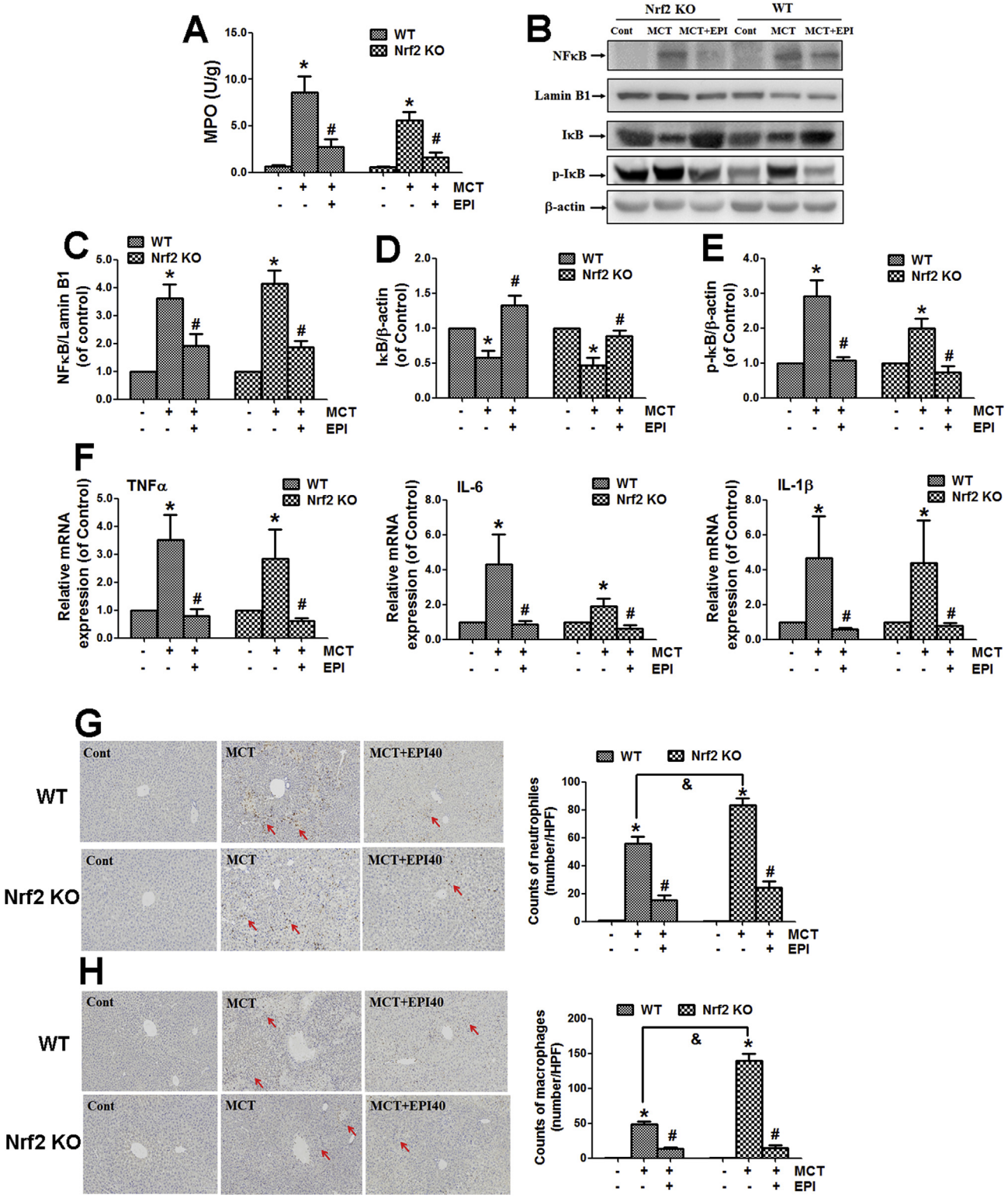

Fig. 7. EPI attenuated MCT-induced liver inflammatory injury in both wild-type and Nrf2 knock-out mice. Wild-type or Nrf2 knock-out mice were given with MCT (360 mg/kg) and EPI (40 mg/kg), and sacrificed at 48 h after MCT administration. (A) Liver MPO activity (n = 6). (B) Hepatic expression of IκB, p-IκB and NFκB. (C) The quantitative densitometric analysis of nuclear NFκB (n = 5). (D) The quantitative densitometric analysis of IκB (n = 5). (E) The quantitative densitometric analysis of p-IκB (n = 5). (F) TNFα, IL-6 and IL-1β mRNA expression (n = 5). (G) Liver immunohistochemical staining of Gr-1. (Arrows indicate Gr-1-positive cells). Left figure is the number of Gr-1-positive neutrophils counted manually (n = 3). (H) Liver immunohistochemical staining of CD11b. (Arrows indicate CD11b-positive cells). Left figure is the number of CD11b-positive macrophages counted manually (n = 3). Data are expressed as mean ± SEM. $^{*}P < 0.05$ versus control; $^{\#}P < 0.05$ versus MCT; $^{\&}P < 0.05$ versus wild-type mice.

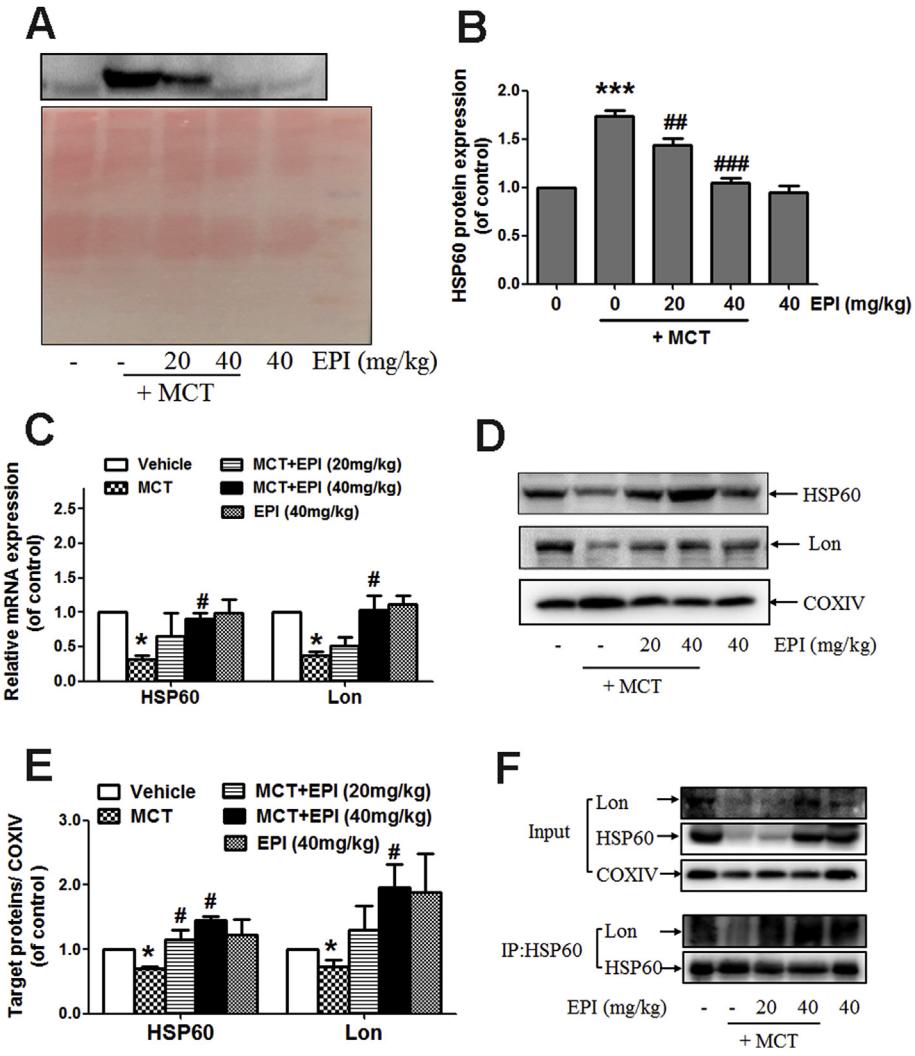

Fig. 8. EPI reduced the release of HSP60 protein induced by MCT. (A) The content of HSP60 in serum from rats. (B) The quantitative densitometric analysis of HSP60 in serum from rats (n = 4). (C) Hepatic mRNA expression of HSP60 and Lon (n = 4). (D) Hepatic mitochondrial HSP60 and Lon expression in rats. (E) The quantitative densitometric analysis of HSP60 and Lon in hepatic mitochondria from rats (n = 4). (F) HSP60 and Lon co-immunoprecipitation assay. Liver mitochondria extracts from rats were subjected to immunoprecipitation with anti-HSP60 antibody and the conjugates were detected with anti-HSP60 and anti-Lon antibodies. Each blot represents one of three independent experiments.

wild-type and Nrf2 knock-out mice.

MCT increased hepatic mRNA expression of tumor necrosis factor (TNF)α, interleukin (IL)-6 and IL-1β in both wild-type and Nrf2 knock-out mice when mice were treated with MCT for 48 h (Fig. 7F). However, all those increases were reversed by EPI in both wild-type and Nrf2 knockout mice.

MCT enhanced the number of Gr-1-staining and CD11b-staining positive immune cells in both wild-type and Nrf2 knock-out mice when mice were treated with MCT for 48 h, but this increase was reduced by EPI in both wild-type and Nrf2 knock-out mice (Fig. 7G and H).

3.8. EPI reduced the release of HSP60 protein induced by MCT

Data in Fig. 8A and B showed that EPI (20, 40 mg/kg) reduced the elevated serum content of HSP60 protein induced by MCT in rats. EPI (40 mg/kg) reversed the reduced mRNA and mitochondrial protein expression of HSP60 and Lon induced by MCT in rats (Fig. 8C–E). Additionally, data in Fig. 7E showed that the binding of HSP60 with Lon protein in mitochondria was decreased in MCT-treated rats, but EPI reversed this decrease.

3.9. Blockage of HSP60 alleviated MCT-induced HSOS in mice

To further confirm the important role of HSP60 in MCT-induced HSOS, mice were injected with anti-HSP60 blocking antibody or control IgG. As shown in Fig. 9A, anti-HSP60 blocking antibody reduced the increased serum ALT/AST activities induced by MCT (360 mg/kg) in mice. Anti-HSP60 blocking antibody also reduced the MCT-induced increase in liver MPO activity (Fig. 9B). The results of liver histological observation demonstrated that livers from mice treated with MCT exhibited serious liver damages, including hepatic infiltration of immune cells, necrosis of hepatocytes and nuclear disappear, endothelial damage of the central vein and sinusoidal hemorrhage (Fig. 9C–b). All those above liver damages were ameliorated by anti-HSP60 blocking antibody (Fig. 9C–c).

After MCT administration (360 mg/kg), the loss of fenestrate organized as sieve plates (only scattered and individual fenestrate are seen) and the formation of large gaps in the sinusoidal endothelium can be observed via scanning electron microscope (Fig. 9D–b). Hepatocytes were exposed and hepatocyte microvilli were visible through those gaps. However, these above liver morphological alterations induced by MCT were improved by anti-HSP60 blocking antibody (Fig. 9D–c).

Next results showed that anti-HSP60 blocking antibody also reduced the MCT-induced increase in hepatic TLR4 expression and nuclear accumulation of NFκBp65 in mice (Fig. 9E and F).

4. Discussion

Although HSOS is not a common liver disease, it is life-threatening. Moreover, now there is still no effective drug for the treatment of HSOS in clinic. A previous study showed that EPI attenuated ionizing radiation-induced liver oxidative injury in mice [22]. Meanwhile, our

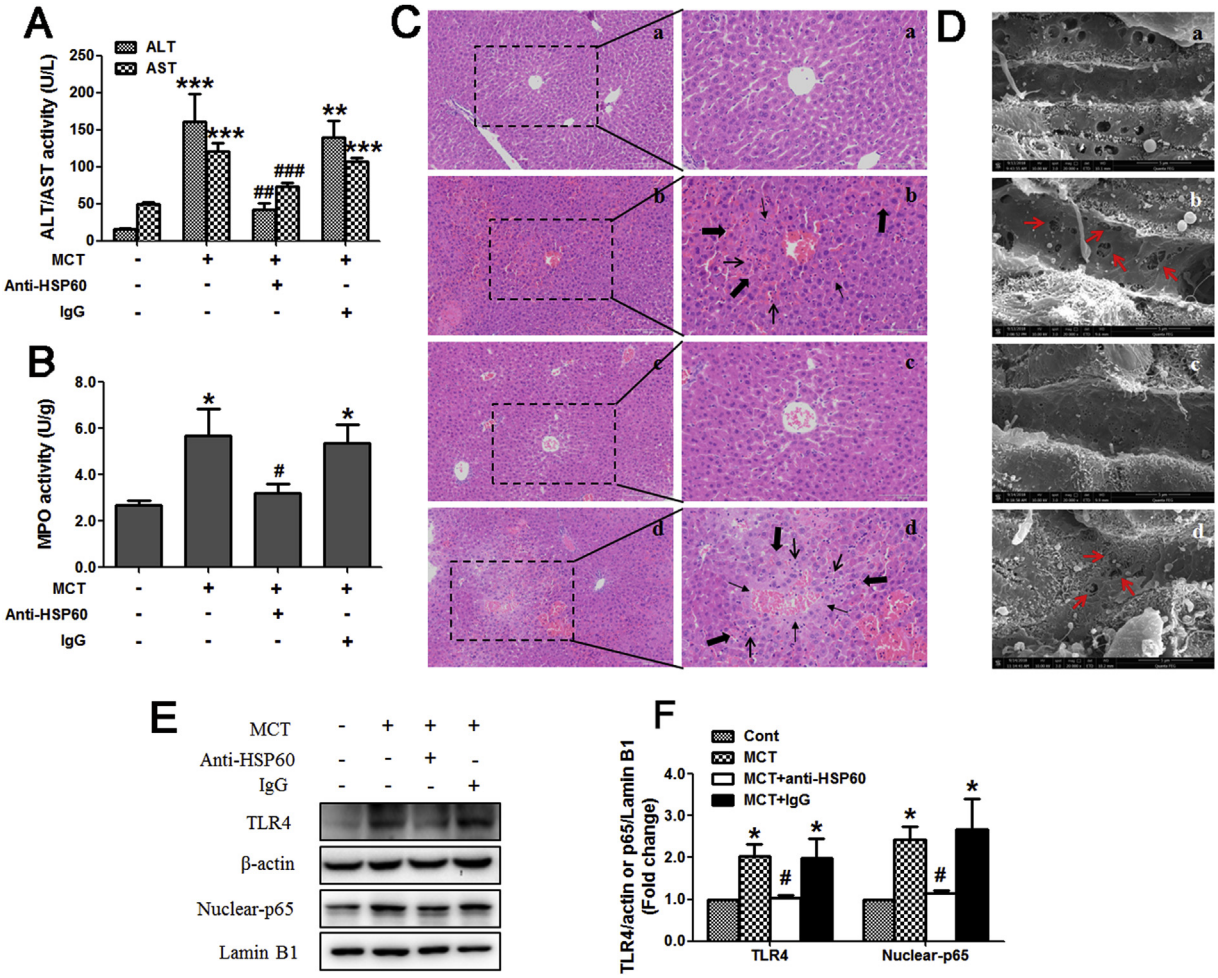

Fig. 9. Blockage of HSP60 alleviated MCT-induced HSOS in mice. (A) Serum ALT/AST activity (n = 5). (B) Liver MPO activity (n = 5). (C) Liver histological evaluation (n = 3). (original magnification, 100× and 200×). The arrows indicate intrahepatic hemorrhage, indicate necrosis of hepatocytes, indicate hepatic infiltration of immune cells. (D) Liver scanning electron microscopy evaluation (n = 3). (original magnification, 20,000 ×). Red arrows indicate the enlargement of fenestrate, exposure of the Disse space and the damage of endothelium. (a) Control. (b) 360 mg/kg MCT. (c) 360 mg/kg MCT + anti-HSP60 antibody. (d) 360 mg/kg MCT + IgG. (E) Liver expression of TLR4 and nuclear NFκBp65. (F) The quantitative densitometric analysis of TLR4 and nuclear NFκBp65 (n = 4). Data are expressed as mean ± SEM. $^{*}P < 0.01$, $^{**}P < 0.01$, $^{***}P < 0.001$versus control. $^{\#}P < 0.05$, $^{\#\#}P < 0.01$, $^{\#\#\#}P < 0.001$ versus MCT.

previous study showed that catechin, another diastereoisomer of catechins, attenuated MCT-induced HSOS in rats by attenuating liver oxidative injury [23]. However, there is still no report about whether EPI also has a protection against HSOS. This study is the first report demonstrated the protection of EPI against MCT-induced HSOS in rats. EPI has already been reported to be safe with no observed adverse effects in healthy volunteers [24]. Thus it can be seen that EPI has the huge prospect to be developed for HSOS treatment in clinic.

EPI was found to enhance liver GSH content, reduce the increased MDA and ROS amounts, and reverse the decreased GST activity induced by MCT in rats. These results imply that EPI can attenuate MCT-induced liver oxidative injury in rats. Nrf2, a key oxidative stress-mediated transcription factor, regulates the expression of a variety of downstream antioxidant enzymes [25]. Nrf2 activation may attenuate the progression of a variety of liver diseases including drug-induced liver injury (DILI), nonalcoholic fatty liver disease (NAFLD) and alcoholic liver disease [26]. Previous studies showed that Nrf2 was involved in the EPI-provided protection against stroke damage, endothelial oxidative stress injury and neurotoxicity [27–29]. Next, we observed whether EPI attenuated MCT-induced liver oxidative injury by activating Nrf2 antioxidant pathway. Firstly, EPI was found to increase Nrf2 nuclear translocation in MCT-treated rats. Secondly, EPI was found to enhance the expression of Nrf2 downstream antioxidant genes including GCLC, GCLM and NQO1. Thirdly, molecular docking analysis indicates the potential interaction of EPI with Nrf2 binding site in Keap1, which is an inhibitor protein for Nrf2 [25]. Finally, when mice were treated with MCT for 24 h, MCT induced serious HSOS in Nrf2 knock-out mice but had no obvious hepatotoxicity in wild-type mice, and the EPI-provided protection against MCT-induced HSOS was totally diminished in Nrf2 knock-out mice. All these above results evidenced the critical role of Nrf2 in preventing MCT-induced HSOS, and the EPI-induced Nrf2 activation contributed to its protection against MCT-induced HSOS.

HO-1 is another important target gene regulated by Nrf2 [26]. MCT enhanced hepatic HO-1 expression in rats, but EPI reduced this increase. The elevated HO-1 expression appears to be an endogenous defensive mechanism used by cells to inhibit inflammation and reduce cell damage, so HO-1 induction is generally seen in a variety of liver injuries [30,31]. Our results imply that the MCT-induced HO-1 expression may be due to the body self-defensive capacity, and EPI-reduced the increased HO-1 expression induced by MCT may be due to the amelioration of HSOS *in vivo*.

Interestingly, EPI obviously attenuated MCT-induced HSOS in Nrf2 knock-out mice when mice were treated with MCT for 48 h. These results indicate that Nrf2 is not critical for the EPI-provided protection against MCT-induced HSOS at the later stage, and there must be other signals contributed to its protection. Previous study showed the linkage

of inflammation with endothelial dysfunction during the development of HSOS [32]. Additionally, the MCT-induced HSOS in rats was reported to be associated with a lobular inflammatory infiltration [11]. In this study, we found that EPI reduced the increased MPO activity, hepatic infiltration of neutrophil and macrophages, and the elevated expression of pro-inflammatory cytokines induced by MCT in both wild-type and Nrf2 knock-out mice when mice were treated with MCT for 48 h. These results indicate that EPI can attenuate MCT-induced liver inflammatory injury.

NFκB is retained in cytoplasm when binding to its inhibitory proteins of IκB family, and the phosphorylation of IκB leads to its degradation and results in the activation of NFκB [33,34]. The NFκB/IκB system plays a critical role in regulating inflammatory responses [33,34]. Our previous studies demonstrated that the inhibition of NFκB activation contributed to the attenuation of HSOS [35,36]. In this study, EPI abrogated NFκB activation induced by MCT in both wild-type and Nrf2 knock-out mice, indicating that EPI attenuated MCT-induced liver inflammatory injury by abrogating NFκB activation.

Heat shock protein 60 (HSP60) is a damage-associated molecular pattern (DAMP), and the elevated release of HSP60 will induce the activation of NFκB and lead to the excessive inflammatory responses [37,38]. To further investigate the mechanism of the EPI-induced abrogation of liver inflammatory injury in MCT-induced HSOS, the effect of EPI on HSP60 expression was observed. Results showed that EPI reduced the elevated serum HSP60 content in MCT-induced HSOS in rats. A previous study showed that the increased expression of Lon, a mitochondrial matrix protein, stabilizes the complex of HSP60-mtHSP70-Lon that leads to the sequestration of HSP60 in mitochondria [39]. Our results showed that EPI reversed the reduced expression of Lon and HSP60 in mitochondria in livers from MCT-treated rats. Additionally, EPI also reversed the reduced interaction of Lon with HSP60. All these results indicate that EPI may reduce HSP60 release by increasing mitochondrial Lon expression, which may contribute to its alleviation on liver inflammatory injury in MCT-induced HSOS in rats.

To further confirm that HSP60 is a key molecule involved in MCT-induced HSOS, anti-HSP60 blocking antibody was used. The results of serum ALT/AST activities, liver histological evaluation and scanning electron microscope observation all evidenced that MCT-induced HSOS in mice was greatly ameliorated by using anti-HSP60 blocking antibody. Furthermore, the MCT-induced activation of TLR4-NFκB signal pathway was also inhibited by anti-HSP60 blocking antibody. These results imply that the activation of NFκB-mediated inflammatory pathway initiated by HSP60 plays an important role in MCT-induced HSOS.

This study showed that EPI ameliorated MCT-induced HSOS by attenuating liver oxidative injury via activating Nrf2 antioxidant pathway and inhibiting liver inflammatory injury via abrogating HSP60-NFκB signaling pathway. Our results suggest that EPI may be a promising therapeutic option for HSOS treatment in clinic.

Conflicts of interest

The authors who have taken part in this study declared that they do not have anything to disclose regarding funding or conflict of interest with respect to this manuscript.

Appendix A. Supplementary data

Supplementary data to this article can be found online at https://doi.org/10.1016/j.redox.2019.101117.

Funding

This work was financially supported by State major science and technology special projects during the 12th five year plan (2015ZX09501004-002-002), the leadership in Science and Technology innovation of the third batch of national “Ten Thousand People Plan” for Lili Ji and National Natural Science Foundation of China (81322053).

References

[1] P. Richardson, E. Guinan, The pathology, diagnosis, and treatment of hepatic veno-occlusive disease: current status and novel approaches, Br. J. Haematol. 107 (1999) 485–493.
[2] P.G. Richardson, et al., Hepatic veno-occlusive disease after hematopoietic stem cell transplantation: novel insights to pathnogenesis, current status of treatment, and future directions, Biol. Blood Marrow Transplant. 19 (2013) S88–S90.
[3] E. Carreras, Veno-occlusive disease of the liver after hemopoietic cell transplantation, Eur. J. Haematol. 64 (2000) 281–291.
[4] J.A. Coppell, et al., Hepatic veno-occlusive disease following stem cell transplantation: incidence, clinical course, and outcome, Biol. Blood Marrow Transplant. 16 (2000) 157–168.
[5] E. Carreras, et al., The incidence of veno-occlusive disease following allogeneic hematopoietic stem cell transplantation has diminished and the outcome improved over the last decade, Biol. Blood Marrow Transplant. 17 (2011) 1713–1720.
[6] P.G. Richardson, et al., Hepatic veno-occlusive disease after hematopoietic stem cell transplantation: novel insights to pathnogenesis, current status of treatment, and future directions, Biol. Blood Marrow Transplant. 19 (2013) S88–S90.
[7] F.C. Willmot, G.W. Robertson, Senecio disease, or cirrhosis of the liver due to senecio poisoning, Lancet 196 (1920) 848–849.
[8] J.Y. Wang, H. Gao, Tusanqi and hepatic sinusoidal syndrome, J. Dig. Dis. 15 (2014) 105–107.
[9] X. Wang, et al., Tusanqi-Related sinusoidal obstruction syndrome in China: a systematic review of the Literatures, Medicine (Baltim.) 94 (2015) e942.
[10] M.J. Tu, et al., Organic cation transporter 1 mediates the uptake of monocrotaline and plays an important role in its hepatotoxicity, Toxicology 311 (2013) 225–230.
[11] L.D. DeLeve, et al., Characterization of a reproducible rat model of hepatic veno-occlusive disease, Hepatology 29 (1999) 1779–1991.
[12] K. Nakamura, et al., Sorafenib attenuates monocrotaline-induced sinusoidal obstruction syndrome in rats through suppression of JNK and MMP-9, J. Hepatol. 57 (2012) 1037–1043.
[13] G. Haklar, et al., Involvement of free radicals in the cardioprotective effect of defibrotide, Arzneimittelforschung 46 (1996) 381–384.
[14] R. Pescador, et al., Defibrotide: properties and clinical use of an old/new drug, Vasc. Pharmacol. 59 (2013) 1–10.
[15] J. Coutsouvelis, et al., Defibrotide for the management of sinusoidal obstruction syndrome in patients who undergo haemopoietic stem cell transplantation, Cancer Treat Rev. 50 (2016) 200–204.
[16] M. Colon, C. Nerin, Role of catechins in the antioxidant capacity of an active film containing green tea, green coffee, and grapefruit extracts, J. Agric. Food Chem. 60 (2012) 9842–9849.
[17] M.A. Islam, Cardiovascular effects of green tea catechins: progress and promise, Recent. Pat. Cardiovasc. Drug Discov. 7 (2012) 88–99.
[18] J. Shay, et al., Molecular mechanisms and therapeutic effects of (-)-Epicatechin and other polyphenols in cancer, inflammation, diabetes and neurodegeneration, Oxid. Med. Cell. Longev. 2015 (2015) 181260.
[19] M. Wei, et al., Natural polyphenol chlorogenic acid protects against acetaminophen-induced hepatotoxicity by activating ERK/Nrf2 antioxidative pathway, Toxicol. Sci. 162 (2018) 99–112.
[20] C. Pang, et al., Caffeic acid prevents acetaminophen-induced liver injury by activating the Keap1-Nrf2 antioxidative defense system, Free Radic. Biol. Med. 91 (2016) 236–246.
[21] L.L. Ji, et al., The involvement of p62-Keap1-Nrf2 antioxidant signaling pathway and JNK in the protection of natural flavonoid quercetin against hepatotoxicity, Free Radic. Biol. Med. 85 (2015) 12–23.
[22] M. Sinha, et al., Epicatechin ameliorates ionizing radiation-induced oxidative stress in mouse liver, Free Radic. Res. 46 (2012) 842–849.
[23] X.Q. Jing, et al., The involvement of Nrf2 antioxidant signaling pathway in the protection of monocrotaline-induced hepatic sinusoidal obstruction syndrome in rats by (+)-catechin hydrate, Free Radic. Res. 52 (2018) 402–414.
[24] C.F. Barnett, et al., Pharmacokinetic, partial pharmacodynamics and initial safety analysis of (-)-Epicatechin in healthy volunteers, Food Funct. 6 (2015) 824–833.
[25] J.W. Kaspar, et al., Nrf2:INrf2 (Keap1) signaling in oxidative stress, Free Radic. Biol. Med. 47 (2009) 1304–1309.
[26] A.M. Bataille, J.E. Manautou, Nrf2: a potential Target for new therapeutics in liver disease, Clin. Pharmacol. Ther. 92 (2012) 340–348.
[27] E.J. Ruijters, et al., The flavanol (-)-epicatechin and its metabolites protect against oxidative stress in primary endothelial cells via a direct antioxidant effect, Eur. J. Pharmacol. 715 (2013) 147–153.
[28] Z.A. Shah, et al., The flavanol (-)-epicatechin prevents stroke damage through the Nrf2/HO1 pathway, J. Cerebr. Blood Flow Metabol. 30 (2010) 1951–1961.
[29] C.C. Leonardo, et al., Oral administration of the flavanol (-)-epicatechin bolsters endogenous protection against focal ischemia through the Nrf2 cytoprotective pathway, Eur. J. Neurosci. 38 (2013) 3659–3668.
[30] G. Sass, et al., The multiple functions of heme oxygenase-1 in the liver, Z. Gastroenterol. 50 (2012) 34–40.
[31] C.S. Origassa, N.O. Camara, Cytoprotective role of heme oxygenase-1 and heme degradation derived end products in liver injury, World J. Hepatol. 5 (2013) 541–549.

[32] A.C. Vion, et al., Interplay of inflammation and endothelial dysfunction in bone marrow transplantation: focus on hepatic veno-occlusive disease, Semin. Thromb. Hemost. 41 (2015) 629–643.
[33] A.B. Lentsch, P.A. Ward, The NFkappaB/IkappaB system in acute inflammation, Arch. Immunol. Ther. Exp. 48 (2000) 59–63.
[34] P.A. Baeuerle, T. Henkel, Function and activation of NF-kappa B in the immune system, Annu. Rev. Immunol. 12 (1994) 141–179.
[35] J.Q. Zhang, et al., Quercetin and baicalein suppress monocrotaline-induced hepatic sinusoidal obstruction syndrome in rats, Eur. J. Pharmacol. 795 (2017) 160–168.
[36] Z.Y. Zheng, et al., Chlorogenic acid suppresses monocrotaline-induced sinusoidal obstruction: the potential contribution of NFκB, Egr1, Nrf2, MAPKs and PI3K signals, Environ. Toxicol. Pharmacol. 46 (2016) 80–89.
[37] X. Liu, et al., Autophagy induced by DAMPs facilitates the inflammation response in lungs undergoing ischemia-reperfusion injury through promoting TRAF6 ubiquitination, Cell Death Differ. 24 (2017) 683–693.
[38] K. Bethke, et al., Different efficiency of heat shock proteins (HSP) to activate human monocytes and dendritic cells: superiority of HSP60, J. Immunol. 169 (2002) 6141–6148.
[39] T.Y. Kao, et al., Mitochondrial Lon regulates apoptosis through the association with HSP60-mtHSP70 complex, Cell Death Dis. 6 (2015) e1642.